

Marquette University

e-Publications@Marquette

---

Biomedical Engineering Faculty Research and  
Publications

Biomedical Engineering, Department of

---

12-2012

## Differential Lung Uptake of $^{99m}\text{Tc}$ -Hexamethylpropyleneamine Oxime and $^{99m}\text{Tc}$ -Duramycin in the Chronic Hyperoxia Rat Model

Anne V. Clough

*Marquette University*, [anne.clough@marquette.edu](mailto:anne.clough@marquette.edu)

Said H. Audi

*Marquette University*, [said.audi@marquette.edu](mailto:said.audi@marquette.edu)

Steven Thomas Haworth

*Medical College of Wisconsin*

David L. Roerig

*Medical College of Wisconsin*

Follow this and additional works at: [https://epublications.marquette.edu/bioengin\\_fac](https://epublications.marquette.edu/bioengin_fac)



Part of the [Biomedical Engineering and Bioengineering Commons](#)

---

### Recommended Citation

Clough, Anne V.; Audi, Said H.; Haworth, Steven Thomas; and Roerig, David L., "Differential Lung Uptake of  $^{99m}\text{Tc}$ -Hexamethylpropyleneamine Oxime and  $^{99m}\text{Tc}$ -Duramycin in the Chronic Hyperoxia Rat Model" (2012). *Biomedical Engineering Faculty Research and Publications*. 65.

[https://epublications.marquette.edu/bioengin\\_fac/65](https://epublications.marquette.edu/bioengin_fac/65)

Marquette University

**e-Publications@Marquette**

***Biomedical Engineering Faculty Research and Publications/College of Engineering***

***This paper is NOT THE PUBLISHED VERSION.***

Access the published version via the link in the citation below.

*Journal of Nuclear Medicine*, Vol. 53, No. 12 (December 2012): 1984-1991. [DOI](#). This article is © Society of Nuclear Medicine and Molecular Imaging and permission has been granted for this version to appear in [e-Publications@Marquette](#). Society of Nuclear Medicine and Molecular Imaging does not grant permission for this article to be further copied/distributed or hosted elsewhere without the express permission from Society of Nuclear Medicine and Molecular Imaging.

# Differential Lung Uptake of $^{99m}\text{Tc}$ -Hexamethylpropyleneamine Oxime and $^{99m}\text{Tc}$ -Duramycin in the Chronic Hyperoxia Rat Model

Anne V. Clough

Department of Mathematics, Statistics and Computer Science, Marquette University, Milwaukee, Wisconsin

Pulmonary and Critical Care Division, Department of Medicine, Medical College of Wisconsin, Milwaukee, Wisconsin

Zablocki VA Medical Center, Milwaukee, Wisconsin

Said H. Audi

Pulmonary and Critical Care Division, Department of Medicine, Medical College of Wisconsin, Milwaukee, Wisconsin

Zablocki VA Medical Center, Milwaukee, Wisconsin

Department of Biomedical Engineering, Marquette University, Milwaukee, Wisconsin

## Steven T. Haworth

Pulmonary and Critical Care Division, Department of Medicine, Medical College of Wisconsin, Milwaukee, Wisconsin

Zablocki VA Medical Center, Milwaukee, Wisconsin

## David L. Roerig

Zablocki VA Medical Center, Milwaukee, Wisconsin

Department of Anesthesiology, Medical College of Wisconsin, Milwaukee, Wisconsin

## Abstract

Noninvasive radionuclide imaging has the potential to identify and assess mechanisms involved in particular stages of lung injury that occur with acute respiratory distress syndrome, for example. Lung uptake of  $^{99m}\text{Tc}$ -hexamethylpropyleneamine oxime (HMPAO) is reported to be partially dependent on the redox status of the lung tissue whereas  $^{99m}\text{Tc}$ -duramycin, a new marker of cell injury, senses cell death via apoptosis or necrosis. Thus, we investigated changes in lung uptake of these agents in rats exposed to hyperoxia for prolonged periods, a common model of acute lung injury. **Methods:** Male Sprague-Dawley rats were preexposed to either normoxia (21%  $\text{O}_2$ ) or hyperoxia (85%  $\text{O}_2$ ) for up to 21 d. For imaging, the rats were anesthetized and injected intravenously with either  $^{99m}\text{Tc}$ -HMPAO or  $^{99m}\text{Tc}$ -duramycin (both 37-74 MBq), and planar images were acquired using a high-sensitivity modular  $\gamma$ -camera. Subsequently,  $^{99m}\text{Tc}$ -macroaggregated albumin (37 MBq, diameter 10-40  $\mu\text{m}$ ) was injected intravenously, imaged, and used to define a lung region of interest. The lung-to-background ratio was used as a measure of lung uptake. **Results:** Hyperoxia exposure resulted in a 74% increase in  $^{99m}\text{Tc}$ -HMPAO lung uptake, which peaked at 7 d and persisted for the 21 d of exposure.  $^{99m}\text{Tc}$ -duramycin lung uptake was also maximal at 7 d of exposure but decreased to near control levels by 21 d. The sustained elevation of  $^{99m}\text{Tc}$ -HMPAO uptake suggests ongoing changes in lung redox status whereas cell death appears to have subsided by 21 d. **Conclusion:** These results suggest the potential use of  $^{99m}\text{Tc}$ -HMPAO and  $^{99m}\text{Tc}$ -duramycin as redox and cell-death imaging biomarkers, respectively, for the in vivo identification and assessment of different stages of lung injury.

## Key Words

acute lung injury; apoptosis; oxidative stress

An essential and lifesaving treatment for hypoxemia in patients with pneumonia or acute respiratory distress syndrome is supplemental  $\text{O}_2$  therapy. However, prolonged exposure to high concentrations of  $\text{O}_2$  can be toxic to the lungs (1-3). Although the mechanisms leading to pulmonary hyperoxic injury are not fully understood, there is ample evidence that the deleterious effects of high  $\text{O}_2$  are the result of increased reactive oxygen species formation, predominantly via mitochondrial pathways (3,4).

The chronic hyperoxia rat model of lung injury mimics key functional aspects of lung  $\text{O}_2$  toxicity observed clinically (1,2,5-7). It is a well-documented acute lung injury model, especially for studies of oxidant-induced lung injury (2,5,6,8,9). Studies by Crapo et al. provide a detailed description of histologic and morphometric changes in the lungs of rats exposed to 85%  $\text{O}_2$  for up to 14 d (6). For the first 72 h of exposure, signs of histologic or morphometric changes are undetectable. By 5 d, there is approximately a 30% loss in capillary endothelial cells and cell surface, infiltration of phagocytic leukocytes and other cell types, and an increase in the thickness of air-blood barrier. By 7 d, the lungs have lost half of the capillary endothelial cells, but pleural effusion and respiratory function impairment have substantially subsided. Capillary endothelial cells that survive 7 d

experience significant morphometric changes including hypertrophy, with substantially less loss of these hypertrophied endothelial cells occurring between 7 and 14 d of exposure (6). These studies suggest that there may be critical biochemical changes in these hypertrophied capillary endothelial cells and reveal that the pulmonary capillary endothelium is a primary target of lung O<sub>2</sub> toxicity.

This sensitivity of the pulmonary capillary endothelium to oxidative stress, and its large surface area and close apposition to blood-borne indicators, have led us and others to develop a range of probes to evaluate the effect of chronic hyperoxia on pulmonary endothelial mitochondrial and cytosolic redox functions (3-5,8,10-12). The utility of these probes is that their pulmonary disposition, metabolism, or redox status is altered after injury or adaptation to hyperoxia (5,8,12). We have developed the use of redoxactive probes that are lipophilic and cell permeant in their reduced form but when oxidized to a less membrane-permeable form become trapped in the cells or sequestered in subcellular organelles (5,8,11). The disposition of these redox probes in the lungs is dependent on the redox state of lung tissue. The redox reactions may occur on either the cell surface or intracellularly, with an end result that the probe is delayed on its passage through the lung vasculature, sequestered in the lung, or both (5,8,10,11). Generally, these experiments have relied on inflow-outflow experiments in isolated perfused lungs using probes that are not suitable for whole-animal experiments and not available in radiolabeled forms suitable for scintigraphy or SPECT. Thus, the overall goal of the present study is to investigate the use of SPECT biomarker imaging in an animal model to detect and delineate particular stages of lung O<sub>2</sub> toxicity injury as a model of human acute lung injury.

<sup>99m</sup>Tc-hexamethylpropyleneamineoxime (<sup>99m</sup>Tc-HMPAO) is a cerebral blood-flow SPECT agent that crosses the blood-brain barrier and is trapped within the brain parenchyma (13). Clinical reports in patients with brain disorders, including psychiatric and movement disorders (13-17) and stroke (18,19), have shown that HMPAO uptake is highly influenced not only by perfusion but also by the nature of the lesion (20,21), suggesting its utility as a biomarker of cell type-specific metabolism. In addition, increases in <sup>99m</sup>Tc-HMPAO uptake in the lungs have been reported in subclinical lung injury due to chemotherapy (22), diffuse infiltrative lung disease (23), irradiation lung injury (24,25), and inhalation and smoking injuries (26-28) in humans. Of particular note is the observation that increases were observed in patients generally showing no abnormal opacity on chest radiographs or findings on pulmonary function tests (22,24,27). Thus, the development of an improved methodology for identifying early lung injury before evidence of structural changes or indirect measures would be an important tool for clinicians treating critically ill patients.

Duramycin is a 19-amino-acid peptide produced by *Streptovorticillium cinnamoneus*. When labeled with <sup>99m</sup>Tc, duramycin acts as a molecular probe for phosphatidylethanolamine, a constituent of the inner leaflet of the plasma membrane (29-31). Generally, phosphatidylethanolamine has little presence on the surface of viable cells, but it becomes exposed with apoptosis, because of the redistribution of phospholipids across the bilayer (29). Duramycin also becomes accessible to the intracellular milieu with necrosis, because of the compromised plasma membrane integrity (29,30). Zhao et al. originally developed <sup>99m</sup>Tc-duramycin as a biomarker for imaging acute cell death in myocardial ischemia/reperfusion injury (30). Rat exposure to 85% O<sub>2</sub> has been reported to result in a significant loss of endothelial cells by 7 d via apoptosis or necrosis as measured by histology (6,32). Such a loss of endothelial cells is consistent with the significant decrease in lung angiotensin-converting enzyme activity, an index of perfused vascular surface area that we have measured in lungs of rats exposed to hyperoxia and used as a measure of change in perfused lung surface area (8). One goal of the present study was to examine the potential for the early detection of oxidative injury to the pulmonary endothelium using the apoptosis-necrosis biomarker <sup>99m</sup>Tc-duramycin. Thus, the aims of this study were to determine the lung uptake of <sup>99m</sup>Tc-HMPAO and <sup>99m</sup>Tc-duramycin in the chronic hyperoxia rat model and to evaluate their potential for the early detection of oxidative lung injury.

## MATERIALS AND METHODS

### Animals

All procedures were approved by the Institutional Animal Care and Use Committees of the Zablocki Veterans Affairs Medical Center. For control animal studies, adult male Sprague-Dawley rats (Charles River Laboratories;  $n = 14$ ; mean body weight  $6 \pm 25.4$  g) were exposed to room air with free access to food and water. For the hyperoxic animal studies, weight-matched rats were housed in a sealed, temperature-controlled ( $22^\circ\text{C} \pm 2^\circ\text{C}$ ) acrylic chamber ( $33.0 \times 58.3 \times 30.5$  cm) maintained at approximately 85%  $\text{O}_2$ , with the balance  $\text{N}_2$ ; free access to food and water; and a 12-h light-dark cycle as previously described (5,8). Bedding, food, and water were changed every other day and the body weight recorded. The total gas flow was approximately 3.5 L/min, and the chamber  $\text{CO}_2$  was less than 0.5%. The animals were then studied after 2 ( $n = 7$ ), 4 ( $n = 9$ ), 7 ( $n = 9$ ), 14 ( $n = 7$ ), and 21 ( $n = 10$ ) days of hyperoxia exposure.

### Imaging

Control normoxic rats and those exposed to chronic hyperoxia were imaged as described below. The rat was anesthetized (pentobarbital sodium [40-50 mg/kg] intraperitoneally), and the left femoral vein was exposed and cannulated with PE-10 tubing attached to an injection syringe containing saline plus heparin (25 units/mL). The rat was then placed supine on an acrylic plate (4 mm) positioned directly on the face of a parallel-hole collimator (hole diameter, 2 mm; depth, 2.54 cm [1 in]) attached to a modular miniaturized g-camera (Radiation Sensors, LLC) with list-mode electronics. Either  $^{99\text{m}}\text{Tc}$ -HMPAO (Ceretek; GE Healthcare) or  $^{99\text{m}}\text{Tc}$ -darmaycin (30) (37-74 MBq), prepared according to kit directions, was then injected via the cannula. The injected dose was calculated from the difference between the pre- and postinjection activity within the syringe using a dose calibrator. Dynamic planar images were acquired every second for the first minute and every minute thereafter for up to 1 h.

Subsequently, without relocation of the animal, an injection of  $^{99\text{m}}\text{Tc}$ -macroaggregated albumin ( $^{99\text{m}}\text{Tc}$ -MAA) (18-37 MBq; particle size, 10-40  $\mu\text{m}$ ; Cardinal Health) was made via the same cannula. The 0.5-mL of  $^{99\text{m}}\text{Tc}$ -MAA injectate consisted of 2.5 mg of aggregated human albumin, 5.0 mg of human albumin, 0.06 mg of stannous chloride, and 1.2 mg of sodium chloride. Ninety-five percent of the  $^{99\text{m}}\text{Tc}$  was bound to the MAA. Images were then obtained at 1 frame per minute for 15 min. Because more than 95% of MAA lodges in the lungs in proportion to flow,  $^{99\text{m}}\text{Tc}$ -MAA is used commonly as a pulmonary perfusion marker (33). However, in these studies, the purpose of the  $^{99\text{m}}\text{Tc}$ -MAA injection was to provide rat thorax images in which the lung boundaries could be clearly identified in the planar images. After imaging, the animals were euthanized with an overdose of pentobarbital sodium.

To determine whether lung uptake of either biomarker is saturable within the amounts used in our study, 4 sequential injections of either  $^{99\text{m}}\text{Tc}$ -HMPAO ( $\approx 37$  MBq/injection) or  $^{99\text{m}}\text{Tc}$ -darmaycin ( $\approx 15$  MBq/injection) were administered to the same control animal and subsequently imaged for 3 min after each injection.

### Image Analysis

First, the boundaries of the lungs were manually outlined in the high-sensitivity  $^{99\text{m}}\text{Tc}$ -MAA images to determine a preliminary lung region of interest (ROI). Then, because HMPAO is taken up substantially by both the liver and the lungs, the lung ROI was truncated by drawing a horizontal boundary at the widest portion of the lung resulting in a lung ROI free of any liver contribution. This  $^{99\text{m}}\text{Tc}$ -MAA lung ROI mask was then superimposed on the time sequence of biomarker ( $^{99\text{m}}\text{Tc}$ -HMPAO or  $^{99\text{m}}\text{Tc}$ -darmaycin) images, yielding lung biomarker ROIs. The resulting mean intraoperator variability in lung uptake measurements was 5.6%, using 4 repeated measurements on 5 different image sets. No registration was required because the animal was maintained in the same location for both the biomarker and the  $^{99\text{m}}\text{Tc}$ -MAA imaging procedures. Background regions in the

upper forelimbs were also identified in the biomarker images to provide a normalization factor. Time-activity curves depicting mean counts per second per pixel per injected dose within the lung and forelimb-background ROIs were then acquired from the time sequence of biomarker images. The ratio of the lung and background ROI curves at each time point was calculated, and the average value over the 10- to 15-min postinjection time interval was used as the measure of lung tissue uptake for each rat (16).

The advantage of the in vivo planar imaging approach used in this study is that the equipment required is now readily available and affordable, and the experimental methods and analysis are straightforward and provide highly sensitive data. Moreover, the use of a subsequent injection of  $^{99m}\text{Tc}$ -MAA to determine the lung boundaries, rather than the use of dual-modality imaging, is an efficient and effective approach that greatly reduces the amount of postprocessing required. The use of  $^{99m}\text{Tc}$ -MAA also provides a unique means of studying regional pulmonary perfusion in models in which blood flow may be altered because of injury or disease. Finally, we acquired planar images throughout the time course of the dynamics of  $^{99m}\text{Tc}$ -HMPAO and  $^{99m}\text{Tc}$ -duramycin lung uptake. Although only the steady-state values of the time-activity curves are reported here, in future studies the complete curve in conjunction with a pharmacokinetic model will be used to further investigate mechanisms involved in hyperoxic lung injury.

## RESULTS

Figure 1 shows the mean of rat body weights at the time of imaging as a percentage of preexposure body weight. Weight loss was greatest at 7 d of exposure to 85%  $\text{O}_2$ , after which the animals began to gain weight. At 21 d of exposure, body weight was significantly higher than at 7 d.

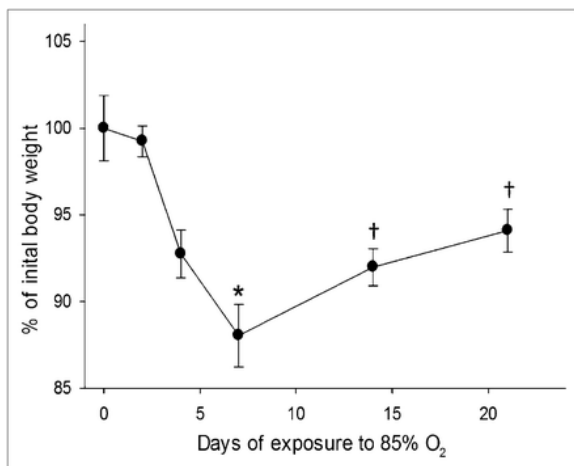


FIGURE 1. Rat body weight at time of imaging study as percentage of preexposure body weight. Values are mean  $\pm$  SE \*Significantly different from control (normoxia),  $P < 0.05$ . †Significantly different from 7 d,  $P < 0.05$ .

A typical planar image of  $^{99m}\text{Tc}$ -HMPAO distribution acquired 10 min after injection is shown in Figure 2A. Figure 2B is an image from the same animal after the  $^{99m}\text{Tc}$ -MAA injection, where lung activity is sufficiently high for reliable identification of the lung boundaries. As described above, the lung ROI from the MAA image was superimposed on the corresponding  $^{99m}\text{Tc}$ -HMPAO image, background ROIs and lung-only ROIs were drawn, and mean background and lung activity were determined.

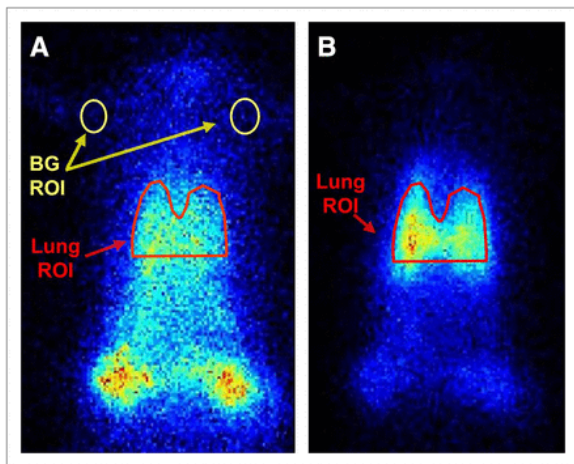


FIGURE 2. Planar images of  $^{99m}\text{Tc}$ -HMPAO (A) and  $^{99m}\text{Tc}$ -MAA (B) distribution in control rat. Lung ROI is determined in  $^{99m}\text{Tc}$ -MAA image and used to identify lung ROI in HMPAO image. Background regions are identified for subsequent calculation of lung-to-background ratio. Lung region above horizontal boundary of ROI is free of any liver contribution. Color indicates counts/s/pixel/MBq injected. BG = background.

The time sequence of images acquired during repeated injections of either  $^{99m}\text{Tc}$ -HMPAO or  $^{99m}\text{Tc}$ -duramycin was analyzed by positioning ROIs over the upper lung and forelimb background regions and computing the difference between the mean lung and background signal at the end of each 3-min acquisition. Lung minus background activity of both  $^{99m}\text{Tc}$ -HMPAO and  $^{99m}\text{Tc}$ -duramycin increased linearly after repeated injections in a control rat (Fig. 3). This linear response indicates that lung uptake of either agent is not saturating and also that incoming photons are not saturating the detection camera or electronics. The linearity is consistent with the lung-to-background ratio being a constant value independent of dose, so that differences in administered  $^{99m}\text{Tc}$ -HMPAO or  $^{99m}\text{Tc}$ -duramycin dose between animals should have no significant effect on the lung-to-background measure of uptake. Lack of saturation with each biomarker within the dose range studied is important for future experiments in which it will be possible to increase the activity of each injection if necessary for adequate sensitivity and count statistics and suggests that when investigating acute responses to lung manipulations, an individual rat may serve as its own control with repeated injections. Furthermore, the protocol could be modified to include an initial injection of  $^{99m}\text{Tc}$ -HMPAO, followed by a subsequent injection of  $^{99m}\text{Tc}$ -duramycin after waiting a sufficient amount of time for  $^{99m}\text{Tc}$ -HMPAO in the lung to reach steady state ( $\approx 15$  min).

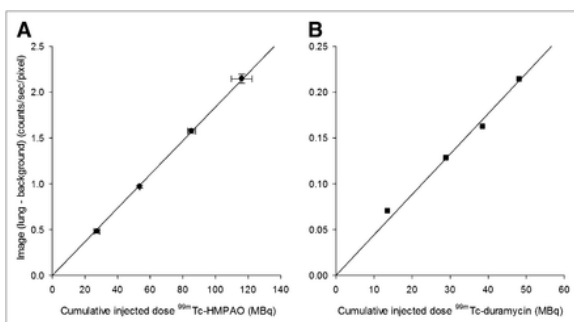


FIGURE 3. Lung (corrected for background) activity measured from images obtained after repeated biomarker injections approximately 3 min apart in control rats. (A) Injections of  $^{99m}\text{Tc}$ -HMPAO ( $\sim 37$  MBq;  $n = 2$ ,  $r^2 = 0.99$ ). (B) Injections of  $^{99m}\text{Tc}$ -duramycin ( $\sim 15$  MBq;  $n = 1$ ).

Figure 4 shows typical  $^{99m}\text{Tc}$ -HMPAO (Fig. 4A) and  $^{99m}\text{Tc}$ -duramycin (Fig. 4B) lung and background time-activity curves obtained from images of control rats. For each biomarker, the first approximately 20 s depict the initial

passage and distribution of the agent in the lung. Figures 4C and 4D depict the ratio of the lung-to-background curves (i.e., lung uptake) at each time point for the data in Figures 4A and 4B, respectively.

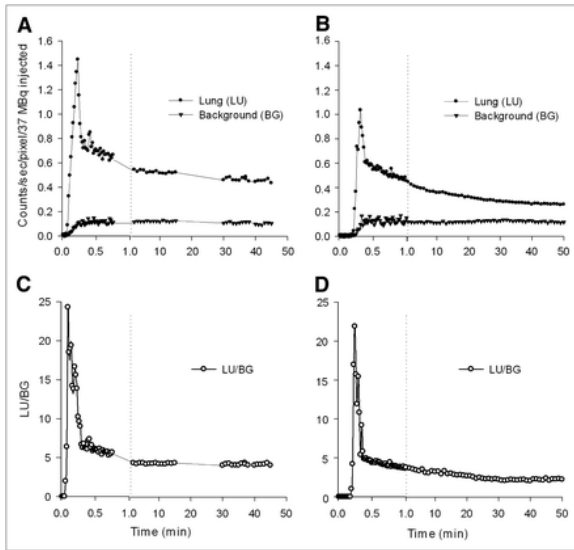


FIGURE 4. Representative time–activity curves acquired from lung and background (upper forelimb) regions of  $^{99m}\text{Tc}$ -HMPAO (A) and  $^{99m}\text{Tc}$ -duramycin (B) planar images of control rats.  $^{99m}\text{Tc}$ -HMPAO (C) and  $^{99m}\text{Tc}$ -duramycin (D) lung uptake calculated as lung-to-background ratio for data in A and B.

Representative images from a control (normoxic) and 7-d hyperoxic rat imaged with  $^{99m}\text{Tc}$ -HMPAO and  $^{99m}\text{Tc}$ -duramycin are shown in Figure 5. Increased uptake of both agents can be observed in the hyperoxic rats. A summary of results of lung uptake for  $^{99m}\text{Tc}$ -HMPAO or  $^{99m}\text{Tc}$ -duramycin for each hyperoxia treatment group as a function of the duration of hyperoxia exposure (number of days) is given in Table 1. Figure 6 shows lung uptake plotted as the percentage change from control as a function of the number days of exposure. Lung uptake of both  $^{99m}\text{Tc}$ -HMPAO and  $^{99m}\text{Tc}$ -duramycin increased significantly up to day 7 of hyperoxia (74% and 51%, respectively). Thereafter,  $^{99m}\text{Tc}$ -HMPAO uptake leveled off whereas  $^{99m}\text{Tc}$ -duramycin accumulation decreased and reached its preexposure value by 21 d. These differences in lung uptake of  $^{99m}\text{Tc}$ -HMPAO and  $^{99m}\text{Tc}$ -duramycin during the course of hyperoxic lung injury may suggest cellular mechanisms involved in both initial injury and subsequent accommodation to the injury.



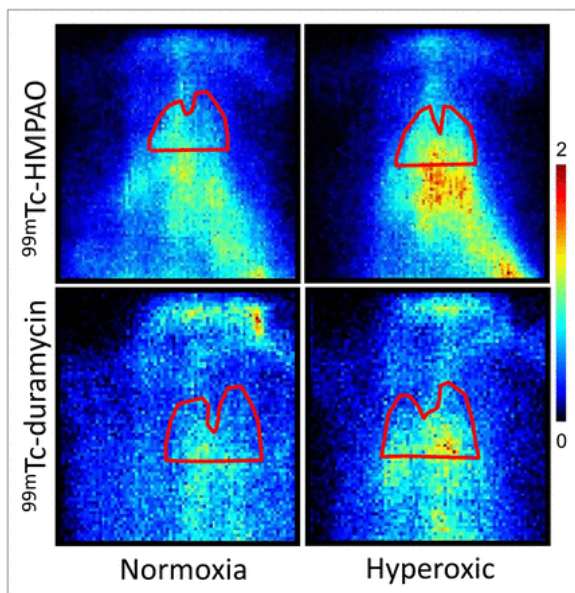


FIGURE 5. Planar images of representative  $^{99m}\text{Tc}$ -HMPAO and  $^{99m}\text{Tc}$ -duramycin distribution in rats. Images were obtained from control (normoxia) and 7-d hyperoxic rats. Lung boundaries were identified using corresponding  $^{99m}\text{Tc}$ -MAA image. Lung region above horizontal boundary of ROI is free of any liver contribution.

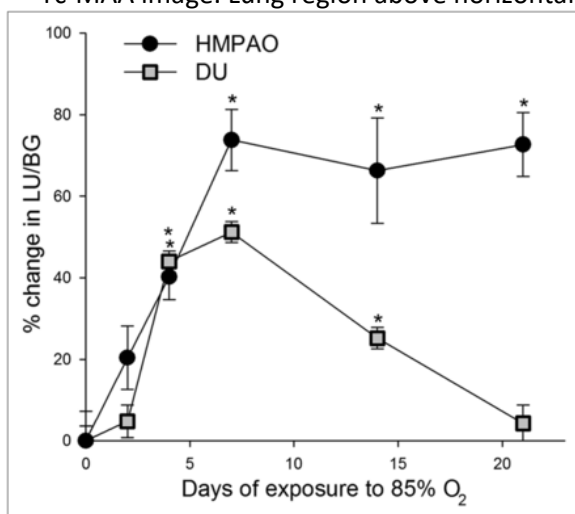


FIGURE 6. Percentage increase from control (normoxia) in  $^{99m}\text{Tc}$ -HMPAO and  $^{99m}\text{Tc}$ -duramycin lung uptake in rats exposed to 85% O<sub>2</sub> for up to 21 d. Values are means  $\pm$  SE. \*Significantly different from control,  $P < 0.05$ . DU = duramycin; BG = background; LU = lung.

**TABLE 1** Effect of Hyperoxia on Lung Uptake (Lung-to-Background Ratio)

Tracer	Control	2 Days	4 Days	7 Days	14 Days	21 Days
$^{99m}\text{Tc}$ -HMPAO	3.79 $\pm$ 0.28 (n = 8)	4.56 $\pm$ 0.35 (n = 3)	5.32 $\pm$ 0.30* (n = 4)	6.59 $\pm$ 0.49* (n = 5)	6.31 $\pm$ 0.81* (n = 4)	6.55 $\pm$ 0.51* (n = 8)
$^{99m}\text{Tc}$ -duramycin	3.21 $\pm$ 0.12 (n = 6)	3.37 $\pm$ 0.14 (n = 4)	4.63 $\pm$ 0.12* (n = 5)	4.86 $\pm$ 0.12* (n = 4)	4.02 $\pm$ 0.11* (n = 3)	3.35 $\pm$ 0.15 (n = 2)

\* $P < 0.05$  when compared with control value.

All data are mean  $\pm$  SE.

## DISCUSSION

Although there is a vast amount of literature on histologic and biochemical changes with hyperoxia lung injury (3,4,6,8), this is the first study, to our knowledge, to evaluate the progression of such lung injury in the hyperoxic rat model using noninvasive in vivo imaging of  $^{99m}\text{Tc}$ -HMPAO or  $^{99m}\text{Tc}$ -duramycin distribution. The hyperoxia-induced increase in  $^{99m}\text{Tc}$ -HMPAO lung uptake measured here is consistent with previous results, which also demonstrate an increase in  $^{99m}\text{Tc}$ -HMPAO uptake in response to pulmonary oxidative stress (oxidant injury), including irradiation lung injury (22,25), inhalation injury (26,27), and cigarette smoking (28). Moreover, this is the first study that we know to report on the pulmonary uptake of  $^{99m}\text{Tc}$ -duramycin in an animal model of disease or injury. The observed changes in the uptake of  $^{99m}\text{Tc}$ -duramycin in this hyperoxia model suggest its potential utility as an in vivo marker of lung cell death.

Rat exposure to chronic hyperoxia resulted in increased lung uptake of both  $^{99m}\text{Tc}$ -HMPAO and  $^{99m}\text{Tc}$ -duramycin; however, and most importantly, the time course of the increase was different for the 2 agents.  $^{99m}\text{Tc}$ -HMPAO uptake in the lung reached a maximum by day 7 and remained elevated out to day 21.  $^{99m}\text{Tc}$ -duramycin uptake also reached a maximum value at day 7 but then decreased at day 14 and returned to a near control level by day 21. These results are consistent with the extensive evidence that 85%  $\text{O}_2$  hyperoxic injury involves an early inflammatory phase (7 d of exposure) characterized by significant loss of capillary endothelial cells, followed by a subsequent adaptation period (6). Thus, the pattern of uptake of these 2 biomarkers has the potential to identify the inflammatory phase of the injury and to provide information on biochemical and structural changes occurring within the lung over the time of exposure to high  $\text{O}_2$  levels.

The mechanisms that determine the lung tissue uptake of HMPAO are still not fully understood (14,19,21,34,35). HMPAO exists in 2 forms, lipophilic and hydrophilic. The more membrane-permeable lipo-form readily diffuses into cells, where it either is sequestered in the cell by conversion to the hydro-nondiffusible form or diffuses back out to the vasculature region. The relative importance of each of these processes to lung tissue uptake of HMPAO remains an open question. Jacquier-Sarlin et al. examined HMPAO retention in several brain cell lines (35). Using D,L-buthionine-sulfoximine and N-acetyl cysteine, chemical agents that decrease or increase, respectively, glutathione content, they showed that the cellular uptake of HMPAO was dependent in part on intracellular glutathione content and thus cell redox status (35). Our previous study demonstrated that rat exposure to 85%  $\text{O}_2$  for 7 d does increase total glutathione content (8). There is also evidence that mitochondrial damage, by reducing metabolic activity, may influence cellular uptake of HMPAO (14,23,34). Our previous studies have also demonstrated a decrease in mitochondrial complex I activity and an increase in mitochondrial complex III and IV activity with hyperoxia exposure (5,8). In addition, studies in brain and muscle cells suggest that the extracellular environment, by modifying the amount of lipophilic HMPAO available to lung cells either by systemic uptake or by conversion of the lipo- to the hydro-form of HMPAO extracellularly, may influence HMPAO cellular uptake (14,35-37).

Another factor that must be recognized when interpreting changes in lung uptake of HMPAO in this hyperoxia model is the significant loss of endothelial cells over the time of exposure—that is, capillary surface area is decreased to approximately 50% and 60% of the control value at 7 and 14 d of exposure, respectively (6). Although our results cannot determine the type of cells that account for the lung tissue uptake of HMPAO, the pulmonary capillary endothelium with its large surface area and direct contact with the blood must certainly play a key role in HMPAO uptake. In addition, imaging measures of uptake are dependent on both the number of cells that take up HMPAO and the amount of HMPAO retained within the cell. Thus, at 7 d of exposure, for example, given the approximately 75% increase in HMPAO lung uptake reported here, and an approximately 50% decrease in capillary surface, it appears that cellular uptake of HMPAO increased by a factor of 3.5, compared with control lungs.

Duramycin binds the head group of phosphatidylethanolamine with high affinity at a molar ratio of 1:1. Phosphatidylethanolamine is available for binding in apoptotic cells because of externalization and in necrotic cells when the plasma membrane is compromised (29,31). Using cultured lymphocytes, Zhao et al. demonstrated a 32 times greater uptake of duramycin in apoptotic cells than in control cells (30). Previous biodistribution studies in the rat showed slight but measurable uptake of duramycin in the lungs of healthy control animals (30), which is consistent with the data presented here. Duramycin uptake in the lungs of hyperoxic rats increased out to 7 d of hyperoxia exposure similar to HMPAO. However, in contrast to HMPAO, duramycin uptake then decreased and was the same as that measured in control animals by 21 d of exposure. In vivo lung uptake of duramycin reported in this study likely reflects overall cell death (32). In fact, the time course of increased duramycin uptake during the hyperoxic lung injury observed here (Fig. 5) appears to parallel the rate of loss of endothelial cells reported previously by Crapo et al. (6) and the loss of body weight of the animals in this study (Fig. 1). Our proposed interpretation of these results is that out to 7 d both HMPAO and duramycin lung uptake in hyperoxic rats increase because of increases in the redox status and apoptosis or necrosis, respectively. After 7 d, the redox status remains high because of the continued high O<sub>2</sub> exposure (high HMPAO uptake), whereas apoptosis or necrosis and the rate of endothelial cell loss decrease (low duramycin uptake). In essence, imaging with these 2 agents has the potential to distinguish both the extent and the different stages of the lung injury.

In this study, we opted to use in vivo planar imaging with a single modular g-camera. The advantage of this approach over full 3-dimensional SPECT is that the equipment required is readily available and affordable and the experimental methods and analysis are straightforward. Moreover, hyperoxic lung injury is thought to be a relatively homogeneous injury throughout the lung so that SPECT would not be expected to provide any additional information about total HMPAO or duramycin retention within the lung. Nonetheless, future studies using 3-dimensional SPECT will facilitate delineation of the entire lung without concern for liver contribution and regional analysis within the lung.

## CONCLUSION

In this study, the effect of hyperoxia on the lung uptake of radiolabeled HMPAO and duramycin was evaluated in vivo. The results suggest that the pattern of the change in biomarker uptake could be useful for differentiating the early inflammatory phase from the subsequent adapted phase of this lung injury model. This delineation is important because patients requiring high O<sub>2</sub> come with differing tolerances of hyperoxia based on genetics, preconditioning, or other factors; real-time information that would permit clinicians to determine which patients are developing O<sub>2</sub> toxicity or tolerance could be of significant value. The results of this study demonstrate substantial uptake of these agents in both normal and injured lung tissue, suggesting their potential clinical utility as pulmonary injury biomarkers. Finally, the approach taken here may be applicable for evaluating the utility of other SPECT biomarkers for assessing lung injury.

## DISCLOSURE STATEMENT

The costs of publication of this article were defrayed in part by the payment of page charges. Therefore, and solely to indicate this fact, this article is hereby marked "advertisement" in accordance with 18 USC section 1734.

## ACKNOWLEDGMENTS

We are grateful to Dr. Ming Zhao (Northwestern University) for producing the duramycin kits and to Drs. Harrison H. Barrett and Lars R. Furenlid (University of Arizona) for providing extensive technical assistance with

the camera hardware and software. This work was supported in part by NIH UL1RR031973, NHLBI 24349, and the Department of Veterans Affairs. No other potential conflict of interest relevant to this article was reported.

## References

1. Capellier G, Maupoil V, Boussat S, Laurent E, Neidhardt A. Oxygen toxicity and tolerance. *Minerva Anestesiol.* 1999;65:388-392.
2. Fisher AB and Beers MF. Hyperoxia and acute lung injury. *Am J Physiol Lung Cell Mol Physiol.* 2008;295:L1066; author reply L1067.
3. Fisher AB, Forman HJ, Glass M. Mechanisms of pulmonary oxygen toxicity. *Lung.* 1984;162:255-259.
4. Brueckl C, Kaestle S, Kerem A, et al. Hyperoxia-induced reactive oxygen species formation in pulmonary capillary endothelial cells in situ. *Am J Respir Cell Mol Biol.* 2006;34:453-463.
5. Audi SH, Merker MP, Krenz GS, Ahuja T, Roerig DL, Bongard RD. Coenzyme Q1 redox metabolism during passage through the rat pulmonary circulation and the effect of hyperoxia. *J Appl Physiol.* 2008;105:1114-1126.
6. Crapo JD, Barry BE, Foscue HA, Shelburne J. Structural and biochemical changes in rat lungs occurring during exposures to lethal and adaptive doses of oxygen. *Am Rev Respir Dis.* 1980;122:123-143.
7. Matute-Bello G, Frevert CW, Martin TR. Animal models of acute lung injury. *Am J Physiol Lung Cell Mol Physiol.* 2008;295:L379-L399.
8. Gan Z, Roerig DL, Clough AV, Audi SH. Differential responses of targeted lung redox enzymes to rat exposure to 60 or 85% oxygen. *J Appl Physiol.* 2011;111:95-107.
9. Ramakrishna M, Gan Z, Clough AV, Molthen RC, Roerig DL, Audi SH. Distribution of capillary transit times in isolated lungs of oxygen-tolerant rats. *Ann Biomed Eng.* 2010;38:3449-3465.
10. Audi SH, Olson LE, Bongard RD, Roerig DL, Schulte ML, Dawson CA. Toluidine blue O and methylene blue as endothelial redox probes in the intact lung. *Am J Physiol Heart Circ Physiol.* 2000;278:H137-H150.
11. Audi SH, Bongard RD, Dawson CA, Siegel D, Roerig DL, Merker MP. Duroquinone reduction during passage through the pulmonary circulation. *Am J Physiol Lung Cell Mol Physiol.* 2003;285:L1116-L1131.
12. Audi SH, Bongard RD, Krenz GS, et al. Effect of chronic hyperoxic exposure on duroquinone reduction in adult rat lungs. *Am J Physiol Lung Cell Mol Physiol.* 2005;289:L788-L797.
13. Catafau AM. Brain SPECT in clinical practice part I: perfusion. *J Nucl Med.* 2001;42:259-271.
14. Gardner A, Pagani M, Beier H, Jacobsson H, Larsson S, Hallstrom T. <sup>99m</sup>Tc- HMPAO distribution at SPECT is associated with succinate-cytochrome c reductase (SCR) activity in subjects with psychiatric disorders. *Nucl Med Biol.* 2004;31:277-282.
15. Habert MO, Horn JF, Sarazin M, et al. Brain perfusion SPECT with an automated quantitative tool can identify prodromal Alzheimer's disease among patients with mild cognitive impairment. *Neurobiol Aging.* 2011;32:15-23.
16. Kaya GC, Ertay T, Tuna B, et al. Technetium-<sup>99m</sup> hexamethylpropylene amine oxime lung scintigraphy findings in low-dose amiodarone therapy. *Lung.* 2006;184:57-61.
17. Nobili F, Koulibaly PM, Rodriguez G, et al. <sup>99m</sup>Tc-HMPAO and <sup>99m</sup>Tc-ECD brain uptake correlates of verbal memory in Alzheimer's disease. *Q J Nucl Med Mol Imaging.* 2007;51:357-363.
18. Eicker SO, Turowski B, Heiroth HJ, Steiger HJ, Hänggi D. A comparative study of perfusion CT and <sup>99m</sup>Tc-HMPAO SPECT measurement to assess cerebrovascular reserve capacity in patients with internal carotid artery occlusion. *Eur J Med Res.* 2011;16:484-490.
19. Oku N, Kashiwagi K, Hatazawa J. Nuclear neuroimaging in acute and subacute ischemic stroke. *Ann Nucl Med.* 2010;24:629-638.
20. Andersen AR, Friberg H, Knudsen KBM, et al. Extraction of [<sup>99m</sup>Tc]-d,l-HMPAO across the blood-brain barrier. *J Cereb Blood Flow Metab.* 1988;8:S44-S51.
21. Inoue K, Nakagawa M, Goto R, et al. Regional differences between <sup>99m</sup>Tc-ECD and <sup>99m</sup>Tc-HMPAO SPET in perfusion changes with age and gender in healthy adults. *Eur J Nucl Med Mol Imaging.* 2003;30:1489-1497.

22. Liu FY, Shian YC, Huang WT, Kao CH. Usefulness of technetium-99m hexamethylpropylene amine oxime lung scan to detect sub-clinical lung injury of patients with breast cancer after chemotherapy. *Anticancer Res.* 2003;23:3505-3507.
23. Hang LW, Shiau YC, Hsu WH, Tsai JJ, Yeh JJ, Kao A. Increased lung uptake of technetium-99m hexamethylpropylene amine oxime in diffuse infiltrative lung disease. *Respiration.* 2003;70:479-483.
24. Suga K, Uchisako H, Nishigauchi K, et al. Technetium-99m-HMPAO as a marker of chemical and irradiation lung injury: experimental and clinical investigations. *J Nucl Med.* 1994;35:1520-1527.
25. Kuo SJ, Yang KT, Chen DR. Objective and noninvasive detection of sub-clinical lung injury in breast cancer patients after radiotherapy. *Eur J Surg Oncol.* 2005; 31:954-957.
26. Hung CJ, Liu FY, Shiau YC, Kao A, Lin CC, Lee CC. Assessing transient pulmonary injury induced by volatile anesthetics by increased lung uptake of technetium-99m hexamethylpropylene amine oxime. *Lung.* 2003;181:1-7.
27. Shiau YC, Liu FY, Tsai JJ, Wang JJ, Ho ST, Kao A. Usefulness of technetium- 99m hexamethylpropylene amine oxime lung scan to detect inhalation lung injury of patients with pulmonary symptoms/signs but negative chest radiograph and pulmonary function test findings after a fire accident: a preliminary report. *Ann Nucl Med.* 2003;17:435-438.
28. ShihWJ, Rehm SR, Grunwald F, et al. Lung uptake of Tc-99m HMPAO in cigarette smokers expressed by lung/liver activity ratio. *Clin Nucl Med.* 1993;18:227-230.
29. Emoto K, Toyama-Sorimachi N, Karasuyama H, Inoue K, Umeda M. Exposure of phosphatidylethanolamine on the surface of apoptotic cells. *Exp Cell Res.* 1997;232:430-434.
30. Zhao M, Li Z, Bugenhagen S. <sup>99m</sup>Tc-labeled duramycin as a novel phosphatidylethanolamine- binding molecular probe. *J Nucl Med.* 2008;49:1345-1352.
31. Zhao M. Lantibiotics as probes for phosphatidylethanolamine. *Amino Acids.* 2011;41:1071-1079.
32. Mantell LL, Horowitz S, Davis JM, Kazzaz JA. Hyperoxia-induced cell death in the lung: the correlation of apoptosis, necrosis, and inflammation. *Ann N Y Acad Sci.* 1999;887:171-180.
33. Bajc M, Neilly JB, Miniati M, Schuemichen C, Meignan M, Jonson B. EANM Committee. EANM guidelines for ventilation/perfusion scintigraphy: Part 1. Pulmonary imaging with ventilation/perfusion single photon emission tomography. *Eur J Nucl Med Mol Imaging.* 2009;36:1356-1370.
34. Fujibayashi Y, Taniudhi H, Waki A, Yokoyama A, Ishii Y, Yonekura Y. Intracellular mechanism of <sup>99m</sup>Tc-d,l-HMPAO in vitro: a basic approach for understanding the hyperfixation mechanism in damaged brain. *Nucl Med Biol.* 1998;25:375-378.
35. Jacquier-Sarlin MR, Polla BS, Slosman DO. Cellular basis of ECD brain retention. *J Nucl Med.* 1996;37:1694-1697.
36. Sasaki T, Toyama H, Oda K, Ogihara-Umeda I, Nishigori H, Senda M. Assessment of antioxidative ability in brain: Tc-99m-meso-HMPAO as an imaging agent for glutathione localization. *J Nucl Med.* 1996;37:1698-1701.
37. Shimura N, Musya A, Hashimoto T, Kojima S, Kuboder A, Sasaki T. Usefulness of <sup>99m</sup>Tc-d,l-HMPAO for estimation of GSH content in tumor tissues. *Nucl Med Biol.* 2000;27:577-580.